Cell-permeant cytoplasmic blue fluorophores optimized for in vivo two-photon microscopy with low-power excitation

ARTICLE *in* MICROSCOPY RESEARCH AND TECHNIQUE · OCTOBER 2007

Impact Factor: 1.15 · DOI: 10.1002/jemt.20493 · Source: PubMed

11 AUTHORS, INCLUDING:

Boudewijn van der Sanden
Clinatec
73 PUBLICATIONS **1,230** CITATIONS
SEE PROFILE

Yves Mély
University of Strasbourg
326 PUBLICATIONS **7,298** CITATIONS
SEE PROFILE

Alain Duperray
French Institute of Health and Medical Resea…
91 PUBLICATIONS **1,958** CITATIONS
SEE PROFILE

Jean-François Nicoud
University of Strasbourg
165 PUBLICATIONS **4,490** CITATIONS
SEE PROFILE

Cell-Permeant Cytoplasmic Blue Fluorophores Optimized for In Vivo Two-Photon Microscopy With Low-Power Excitation

ALI HAYEK,[1] ALEXEI GRICHINE,[2] THOMAS HUAULT,[3] CLÉMENT RICARD,[4]
FRÉDÉRIC BOLZE,[1] BOUDEWIJN VAN DER SANDEN,[5] JEAN-CLAUDE VIAL,[3]
YVES MÉLY,[6] ALAIN DUPERRAY,[7,8] PATRICE LILIAN BALDECK,[3] AND JEAN-FRANÇOIS NICOUD[1]*
[1]*Institute of Physics and Chemistry of Materials of Strasbourg, Organic Materials Group, CNRS and Université Louis Pasteur-Strasbourg I (UMR 7504), 23 rue du Loess, 67034 Strasbourg, France*
[2]*University Joseph Fourier-Grenoble I, Institute Albert Bonniot – IFR 73, Platform "Optical microscopy–cell imaging," BP 170, La Tronche, 38042 Grenoble Cedex 9, France*
[3]*Laboratoire de Spectrométrie Physique, CNRS and Université Joseph Fourier-Grenoble I (UMR 5588), BP 87, 38402 Saint Martin d'Hères, France*
[4]*INSERM U594 "Functional and Metabolic Neuroimaging," Academic Hospital of Grenoble, Pavillon B, BP 217, 38043 Grenoble, France*
[5]*INSERM U647 "Medical Applications of Synchrotron Radiation", European Synchrotron Radiation Facility, 6 rue Jules Horowitz, 38043 Grenoble, France*
[6]*Institut Gilbert Laustriat, CNRS (UMR 7175), Faculté de Pharmacie, 74, route du Rhin, BP 60024, 67401 Illkirch-Graffenstaden, France*
[7]*INSERM U578, 38706 Grenoble, France*
[8]*Université Joseph Fourier-Grenoble I, Groupe de Recherche sur le Cancer du Poumon, Institut Albert Bonniot, (IFR 73), La Tronche 38706 Grenoble, France*

KEY WORDS two-photon dyes; cell microscopy; FLIM; FRAP; photostability; mouse brain imaging; BBB

ABSTRACT Because of the spreading of nonlinear microscopies in biology, there is a strong demand for specifically engineered probes in these applications. Herein, we report on the imaging properties in living cells and nude mice brains of recently developed water soluble blue fluorophores that show efficient diffusion through cell membranes and blood–brain barriers. They are characterized by two-photon absorption cross-sections of 100–150 Goeppert-Mayer range in the near IR and fluorescence efficiencies of up to 72% in water. They were found to stain homogeneously the cytoplasm of cultured living cells within minutes. Moreover, their diffusion times and fluorescence characteristics in the cytoplasm suggest a hydrophobic association with intracellular membranes. Their intracellular fluorescent decays were found to be almost mono-exponential, a very favorable feature for fluorescence lifetime imaging. Two photon images of living cells were obtained with a good signal to noise ratio using laser powers in the sub-milliwatt range. This allows continuous imaging without significant photobleaching for tens of minutes. In addition, these fluorophores allowed in vivo three-dimensional two-photon imaging of mice cortex vasculatures and extra vasculature structures, with no sign of toxicity. *Microsc. Res. Tech. 70:880–885, 2007.*

INTRODUCTION

During the last decade, nonlinear optical microscopies have spread in biological laboratories. Laser scanning microscopies based on two-photon excited fluorescence (TPEF) and second-harmonic generation are readily obtained with commercial turnkey femtosecond lasers and confocal microscopes (Bousso and Robey, 2004; Imanishi et al., 2004; Miller et al., 2002; So et al., 2000; Xu et al., 1996; Zipfel et al., 2003). In most cases, the labeling molecules are standard fluorescent dyes that do not exhibit optimized nonlinear optical properties. Many organic chemistry groups are regularly reporting on efficient nonlinear optical chromophores for different applications including bio-imaging. However, only a few of such nonlinear molecules can be used for cellular and in vivo imaging due to the specific constraints that are required: solubility and fluorescence in water, membrane-crossing properties, non toxicity, and photostability (Abbotto et al., 2002, 2005; Krishna et al., 2006; Woo et al., 2005). Blue-fluorescent probes are attractive for multicolor fluorescence applications in vivo as they provide a complementary labeling color to the commonly used green, yellow, orange, or red fluorescent proteins and probes. Two-photon excitation provides an important alternative to ultra-violet excitation lines, since it reduces the endogenous fluorescence and causes less photodamage. In addition, the same two-photon excitation wavelength, and there-

*Correspondence to: Jean-François Nicoud, Institute of Physics and Chemistry of Materials of Strasbourg, Organic Materials Group, CNRS and Université Louis Pasteur-Strasbourg I (UMR 7504), 23 rue du Loess, 67034 Strasbourg, France. E-mail: nicoud@ipcms.u-strasbg.fr

Received 11 January 2007; accepted in revised form 22 March 2007

DOI 10.1002/jemt.20493

Published online 27 July 2007 in Wiley InterScience (www.interscience.wiley.com).

fore the same excitation volume, can be used for a large range of multicolor probes. The main blue fluorescent dye used actually in TPEF microscopy of living cells is Hoechst 33342 that stains specifically nucleic acids. Other blue emitting dyes, such as DAPI, cascade blue, alexa fluor 350, AMCA, or dansyl chloride are used on fixed specimens, and often in the form of bioconjugates. These blue fluorophores exhibit low two-photon absorption (TPA) cross-sections in the Goeppert-Mayer (GM) range (Xu et al., 1996) and can thus hardly be used for sensitive two-photon imaging.

TPEF microscopy is a powerful technique to obtain three-dimensional images of diffusing tissues (Helmchen and Denk, 2005). In particular, brain angiography at the cellular scale is possible by injecting intravenously TPEF chromophores (Serduc et al., 2006; Vérant et al., 2006) or multicell bolus loading technique (Göbel et al., 2006). Recently, multicolor injection of green FITC-Dextran and red sulforhodamine B allowed a differential intravital imaging in the mouse brain that revealed radiotherapy cellular damages (Vérant et al., 2006). More generally, new multichannel TPEF molecules able to cross the blood–brain barrier (BBB) and probe the cell activity would be needed to study the brain functions at the cellular level.

We have previously reported on the design, preparation, and photo-physical properties of water soluble blue-fluorescent dyes with high TPA cross-sections (Hayek et al., 2006). These dyes are composed of two stilbenic units linked by a single carbon–carbon σ bond. Oligoethyleneglycol chains have been grafted at molecule ends to provide good water solubility. These dyes are neutral analogs of "Stilbene-420" that is known to be a nontoxic, highly fluorescent, and photobleaching resistant laser dye.[1]

In this work, we have investigated the imaging properties of these enhanced-TPA blue fluorophores in living cells and nude mice brains. TPEF intensity, fluorescence recovery after photobleaching (FRAP), and fluorescence lifetime imaging (FLIM) microscopies have been used to characterize their cytoplasmic localization, accumulation kinetics, association and diffusion properties, and photobleaching resistance, as a general method of investigation for newly engineered TPEF dyes for biological imaging. Moreover, in vivo three-dimensional TPEF imaging has been used to evaluate the staining of vasculatures and extra vasculature structures in the cortex of nude mice, this last point evidencing diffusion through the BBB.

MATERIALS AND METHODS

Chemicals

Chromophores **1** and **2** were prepared as previously described (Hayek et al., 2006). The first one is built around a biphenyl central core, and the other one, on a fluorenyl moiety leading to a blocked planar geometry of the entire molecule (Fig. 1).

Cell Culture and Staining Procedure

Adherent Chinese Hamster Ovary (CHO), Cos7 (Simian fibroblasts), Hela (human carcinoma), NIH/3T3 (mouse fibroblasts), and F98 (rat glioma) cells were cultured in complete culture medium (DMEM containing 10% FBS, 2 mM L-Glutamine, 100 U/mL penicillin, 100 μg/mL streptomycin, and nonessential amino acids (BioWhittaker)). Twenty-four hours before experiments, cells were plated on LabTek chambered cover glass (Nunc) in complete culture medium. At the beginning of the experiment about 50% confluence was obtained. A small quantity of concentrated water stock solutions of **1** and **2** was first diluted 100 times in complete culture medium and then mixed with an equal quantity of medium in a LabTek chamber to obtain a final concentration of 5×10^{-6} M and homogeneous initial distribution of the dye. No rinsing was made before measurements.

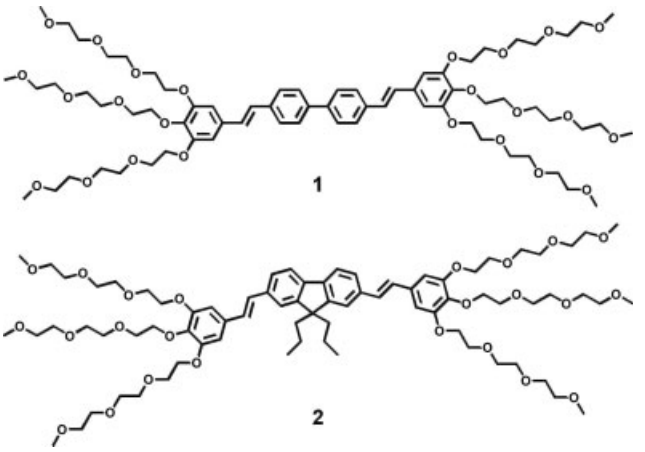

Fig. 1. Molecular structures of chromophores **1** and **2**.

Two-Photon Microscopy (3D Intensity Imaging, FRAP, and FLIM) on Cells

Two-photon microscopy on cultured cells was performed with an inverted two-photon laser scanning microscope Axiovert 200 (LSM510 NLO, Carl Zeiss) equipped with pulsed IR femtosecond Ti:Sapphire laser (Tsunami, Spectra-Physics). The excitation wavelength was tuned to about 730 nm with pulse duration of 150 fs. The irradiation intensity on the sample was 700 μW at 2% transmission of the acousto–optical tunable filter (AOTF). The fluorescence of **1**, **2**, and Hoechst 33342 was selected with the same 390–465 nm emission band-pass filter. All measurements were performed using a 63x/1.4 oil immersion plan-apochromat objective. Cells were maintained at 37°C in a humidified atmosphere containing 5% CO_2.

For the characterization of the accumulation kinetics, the applied laser intensities were adjusted to 7% of the available power for the compound **1** and 2 % for **2** in order to avoid bleaching effects and obtain a good signal to noise ratio. For the sake of comparison, the curves in Figure 4 were normalized to the same excitation intensity. Supposing the squared excitation efficiency with two photons, the intensities of **1** were divided by a factor of 12.25.

In FRAP experiments, cells were incubated with each product for 30 min in complete culture medium. A circular region of 3 μm diameter was then bleached with a high laser intensity in the homogeneous region

[1] "Stilbene 420," also called "stilbene 3", is 2,2"-([1,1′-biphenyl]-4.4′-diyldi-2,1-ethenediyl)bis-benzenesulfonic acid disodium salt (CAS N° 27344-41-8).

of the cytoplasm and the images were taken each 2 s. Care was taken to not induce cell heating or damage with excessive laser power.

For FLIM experiments, the fluorescence decays were measured by the time correlated single photon counting (TCSPC) technique. A single photon counter (photomultiplicator tube, PMT H7422-P, Hamamatsu) was coupled to the nondescanned detection port of the two-photon microscope. The photon counts of fluorescence were amplified and registered with a SPC830 counter (Becker&Hickl). Each count was synchronized with the following excitation pulse of the 80 MHz Ti:Sapphire laser as well as with pixel, line and frame clocks from the microscope scanning head. The mean count rate was chosen to be at least three orders of magnitude lower than the laser repetition rate by decreasing the excitation power in order to avoid the pulse pileup artifacts, even in the regions of high concentration. Acquisition time for a typical image 256 × 256 pixels was 3 min with a mean count rate about 65 kHz.

Two-Photon Microscopy on Mice

Mice of 6 weeks ($n = 2$) and 8 months ($n = 2$) of age were anesthetized with a gas mixture of 2% isoflurane in 30% O_2 and 68% N_2 and placed on a stereotaxic frame. A craniotomy of 3 mm in diameter was carried out on the top of the left parietal cortex. A 100-μL solution of compound **2** (10 mg/mL) was injected in the tail vein of mice. Core temperature was maintained at 37°C using warm water circulating through a pad and the head of the mice was positioned under a 20× water immersion objective.

Two-photon laser scanning microscopy in vivo was performed with a confocal microscope consisting of a Biorad (MRC 1024) scanhead and an Olympus BX50WI microscope. A 800-nm excitation beam from a femtosecond Tsumami Ti:Sapphire laser (5-W pump; Spectra-Physics, Millenia V) was focused into the sample using a 20× water-immersion objective (0.95 numerical aperture, Xlum Plan FI Olympus) and the beam was scanned in the x–y plane to acquire a 512 × 512 image (0.9 s/image).[2] The z-scan (variation of the observation depth) was realized by translation of the motorized objective. The incident laser intensity was varied by using a polarizer in front of the microscope so that the total average power delivered at the surface ranged from 20 to 200 mW (see Vérant, 2006 for details). For the experiments carried out here, the confocal configuration was not used and the nondescanned fluorescence was collected with two added external PMT protected by a BG39 filter (Schott Glass – Jena) associated with a 710 ASP blocking filter (Omega-filters Corp).

Image acquisition and reconstruction were performed using the Biorad exploitation system. Planar scans of the fluorescent intensity were acquired at successive depths in the cortex. The z-step between scans was 1–2 microns. Acquisition of a stack took 1–2 min. Images were analyzed using Image J and a home-made software.[3]

[2]The Tsunami laser is known to have a beam shift when spectrally tuned, we have taken care of this problem.

[3]ImageJ. v.1.33 Public Domain Software, available on http://rsb.info.nih.gov/ij/, 2005.

TABLE 1. Photophysical properties of chromophores **1** *and* **2** *in water and dichloromethane*

	One-photon abs.[a]		Two-photon abs.[a]		Emission		
	λ_{max} (nm)	ε (M^{-1} cm^{-1})	λ_{max} (nm)	σ_2 (GM)	λ_{max} (nm)[a]	ϕ[a]	τ (ns)[b]
H_2O							
1	357	62,000	720	110	450	39	7.1 (43 %) 1.7 (50 %) 0.25 (7 %)
2	383	58,000	720	160	453	72	3.25 (75 %) 0.15 (25 %)
CH_2Cl_2							
1	362	73,000	720	110	439	75	1.12
2	382	81,000	720	160	450	81	1.26

[a]From Hayek et al., 2006.
[b]From this work.

RESULTS

Structure and Properties of Fluorophores

The structures of chromophores **1** and **2** used during these studies are shown in Fig. 1. Both chromophores are highly water soluble (200 and 90 g/L at room temperature, respectively for **1** and **2**). Their octanol–water partition coefficients (log$P$) are 1.9 and 1.5 for **1** and **2**, respectively (turbidimetric method) (Hayek et al., 2006).

The fluorescence properties of dyes **1** and **2** in water and dichloromethane are summarized in Table 1. These dyes are efficient blue ($\lambda_{em} \approx 450$ nm) fluorophores that can be excited either by one photon absorption in the UV or by two-photon absorption in the near infrared range. In particular, the fluorescence quantum yields are 39% and 72% for **1** and **2**, respectively in water. Their TPA cross-sections are around 100–150 GM in the near IR at 700 nm, which are almost two orders of magnitude larger than those of commercial blue fluorophores. Moreover, their fluorescence lifetimes are mono-exponential in a hydrophobic environment, a feature that is favorable for intracellular FLIM imaging (Table 1).

Additional experiments were carried out with **1** and **2** dissolved in a 1% water suspension of Triton X-100 micelles. This simple system constitutes a useful model for the hydrophobic interactions of drugs in vivo (Grichine et al., 2001). The fluorescence decays were found to be monoexponential with a lifetime of 1.1 ns (**1**) and 1.2 ns (**2**). The fluorescence quantum yield of compound **1** (27%) in micelles was lower than that in water (Table 1) while that of **2** was higher (84%). The emission maximum of **2** in micelles was around 442 nm and was thus blue shifted as compared to water.

Accumulation Kinetics and Distribution of Fluorophores in Cells

Both compounds **1** and **2** were found to penetrate rapidly and accumulate in a large panel of living animal and human cells (CHO, F98, HeLa, Cos7, or NIH/3T3). The distribution of the dyes was homogeneous in the cytoplasm (Fig. 2a) and no accumulation in the nucleus was detected. The fluorescence emission maximum of **2** was 442 nm as in micelles. More generally, the intracellular fluorescence characteristics of both compounds are similar to those in Triton X-100 micelles (see also FRAP and FLIM results), suggesting an accumulation in an environment where the compounds hydrophobically interact with low polar cell

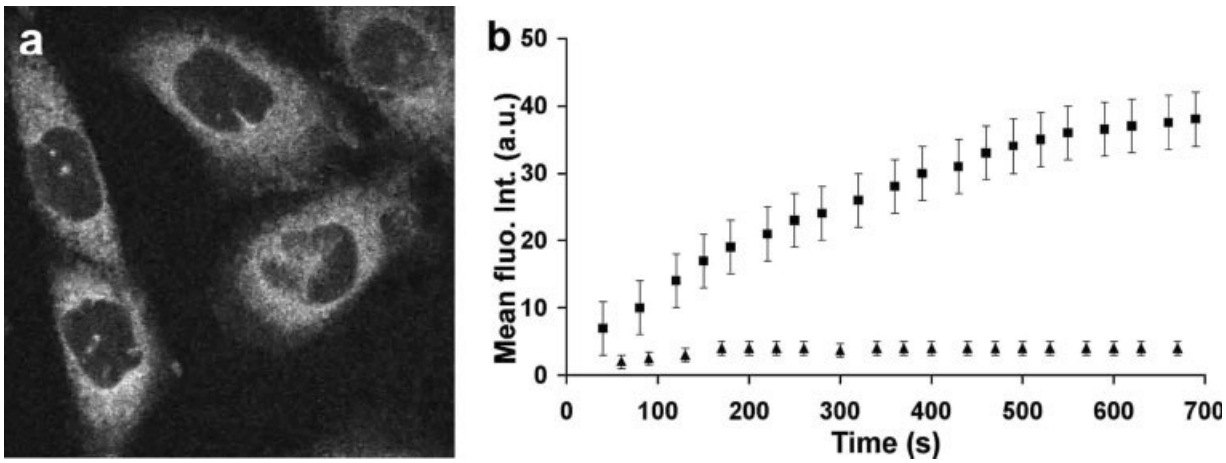

Fig. 2. (**a**) The typical distribution pattern of **2** in living CHO cells after 10 min incubation in complete culture medium containing 5 μM of the dye. (**b**) Uptake of **1** (triangles) and **2** (squares) measured as the average intensity in the cytoplasm of 10–15 cells. No detectable photobleaching effects were induced during measurements as compared to the intensities in the neighboring regions. Curves were normalized to the same excitation power (2% AOTF transmission).

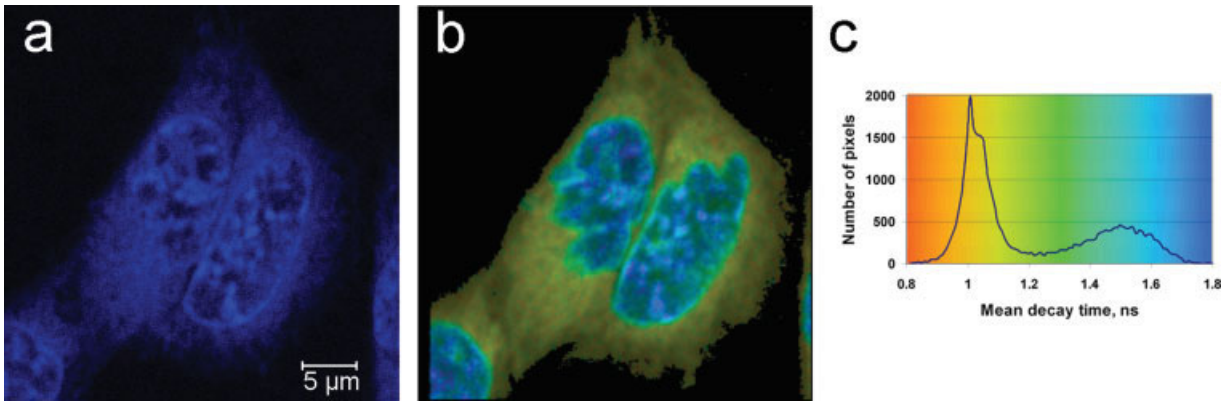

Fig. 3. (**a**) TPEF image of **2** and Hoechst 33342 in living CHO cells. (**b**) FLIM image of the same cells measured by the TCSPC method. (**c**) Lifetime distribution histogram of the FLIM. The two peaks correspond to the fluorescence lifetime distributions of **2** and Hoechst 33342, respectively.

components. The fluorescence level of **2** in the cytoplasm was about 10 times higher than that of **1** after 10 min incubation as shown in Figure 2b. The fluorescence signal is proportional to the TPA cross-section, the compound concentration and its fluorescence efficiency. The TPA cross-section of **2** is 1.5 times higher than that of **1** and, in the micelle environment, the fluorescence quantum yield of **2** is 3 times higher than that of **1**. Therefore, the cytoplasmic concentration of compound **2** is estimated to be about 2 times higher than that of compound **1**.

Accumulation kinetics was characterized with CHO cells. The 50% accumulation of **1** was reached in 1 min and that of **2** in 4.5 min. Similar differences in the uptake efficiencies of **1** and **2** were observed on other cell lines, such as Cos7 and NIH3T3. These differences in the accumulation kinetics of **1** and **2** can not be explained solely by their difference in log*P*, since the membrane permeability of related molecules varies linearly with their partition coefficient. Because of its PEG and alkyl chains, compound **2** likely forms micelles (dialysis data not shown). As a consequence, its slower kinetics and more efficient accumulation in these cells could be due to the internalization of these micelles by endocytosis.

Cytoplasmic Diffusion Measurement by FRAP

To compare the cytoplasmic diffusion of **1** and **2**, we performed FRAP experiments in CHO cells. The recovery times of **1** and **2** were found to be identical within experimental errors: $\tau_{1/2} = 7 \pm 1$ s. This diffusion is much slower than expected for free molecules in the cytoplasm, for example the recovery time of free cytoplasmic GFP in identical conditions is of the order of 0.1 s. Therefore, compounds **1** and **2** are probably associated with cellular structures in the cytoplasm. Since the spectroscopic characteristics of both dyes in cells are similar to those in micelles, the dyes likely interact with intracellular membranes.

Cytoplasmic Fluorescence Lifetimes and FLIM Imaging

Measurement of the fluorescence decays in living CHO cells yielded a mean fluorescence lifetime of 0.9 ±

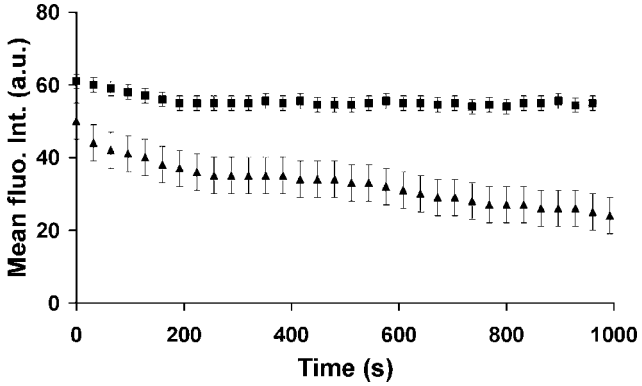

Fig. 4. Time course of the mean fluorescence intensity in the cytoplasm of living CHO cells. **1** (triangles) was excited with 7% AOTF transmission, and **2** (squares) was excited with 2% at 730 nm. The pixel dwell time was 6.4 μs, each line was averaged four times and successive images were taken each 6.5 s. Each data point corresponds to the mean fluorescence intensity in the cytoplasm of several cells. Each fifth time point is shown for clarity.

0.1 ns for compound **1** and 1.0 ± 0.1 ns for **2**. The fluorescence decays were almost single exponentials for both compounds. The distribution of lifetime values was rather homogeneous throughout the cytoplasm (Fig. 3). One should notice that the accuracy of the measurements was limited mostly by the nature of the specimen rather than by the detection system. Indeed, living cells inherently move during the acquisition time (about 3 min/image), inducing small local changes in the microenvironment of individual fluorophores. Thus, the time-independent model used here is only an approximation of the real fluorescence decays in each pixel. The mean decay values measured in the cytoplasm are much smaller than those measured in aqueous buffer (Table 1) and close to the values observed in low polar solvents and in the model Triton X-100 system. This further supports the hypothesis of hydrophobic interactions of **1** and **2** with cellular membranes.

Photobleaching Experiment

Under UV excitation, both compounds exhibit similar photobleaching rates (data not shown) due to their similar molecular structures. In Figure 4, we report the photobleaching resistance of both dyes in the typical conditions of two-photon imaging in cultured cells. The average power on the sample was 2.5 mW for **1** and 0.7 mW for **2** to obtain similar signal intensities. After an initial decrease during 1 min of acquisition, the fluorescence intensity of **2** stabilized at about 90% level whereas that of **1** decreased continuously. This higher bleaching rate of compound **1** may result from highly nonlinear dependence of 2P photobleaching on the excitation power (Patterson and Piston, 2000). Even though both substances are subject to photobleaching, the higher TPA cross-section and accumulation level of **2** allow the use of lower laser intensity and limit the photobleaching during cell imaging. Compound **2** was sufficiently stable to be continuously imaged with high S/N ratio for up to 17 min without significant photodegradation. This feature will enable the detailed analysis of **2**-labeled biomolecules in future applications.

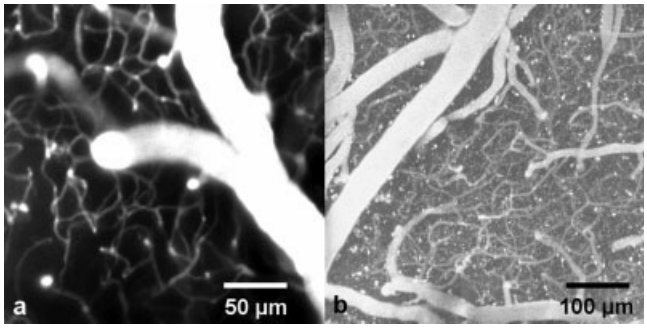

Fig. 5. (**a**) *z*-projection of 100 pictures acquired from 0 to 100 μm below the dura after an intravenous injection of chromophore **2** in a 6-weeks-old mouse. (**b**) *z*-projection of 100 pictures acquired from 0 to 200 μm below the dura after an intravenous injection of chromophore **2** in an 8-months-old mouse. Raw data were treated with the rolling ball algorithm of the ImageJ software using a radius of 50 pixels.

Cell Survival

The cytotoxicity of fluorophores **1** and **2** was evaluated over a 1 week period using CHO cells. After incubation with very high concentrations of fluorophores (10^{-4} M), cells continued to grow normally and became confluent with the same kinetics as control cells. Neither the presence of the dye inside cells nor its two-photon excitation resulted in any visible alteration of cell morphology (data not shown). Thus, these compounds did not show any sign of cytotoxicity.

In vivo Two-Photon Microscopy on Mice Brain

Results of the cerebral vasculature staining in the cortex of nude mice using chromophore **2** are shown in Figure 5. This figure has been obtained under conditions that are used for efficient dyes, that is, an acquisition time of 1 s/slice and a moderate laser illumination in order to keep the animal in good physiological conditions ($\approx$10 mW average power at the focus point). An efficient staining is obtained for large vessels as well as for capillaries indicating an homogeneous distribution of the dye. The chromophore **2** was observable until a depth of 200 μm beneath the dura. Mice stayed alive after intravenous injection of the chromophore **2** and for the duration of the whole experiment of maximum 4 h. It should be noted that for this focussing depth, the laser does not induce a measurable endo- or exo-luminescence at the surface of the dura, at the opposite of what has been mentioned by Theer and Denk (2006).

Figure 5a has been obtained for a 6-weeks-old mice, the capillaries were contrasted on a black background, which indicated a strictly intravascular staining. On the contrary, in mice at 8 months of age, extra vascular structures were stained in $\sim$20 min after injection (Fig. 5b). The size of stained structures varied in between 3 and 10 μm. Their density was more important at the top of cortex Layer II, which is known to have a higher cell density. We hypothesize that these structures are intracellular (see previous results on Cell Cultures), but further histochemical analysis is necessary to elucidate the nature of this staining.

The hydrophilic moieties in the dye enable a high concentration in the blood. Moreover, the lipophilic moieties as well as the nonionic nature of the chromo-

phore favor the diffusion across the BBB. These results are encouraging since the dye assimilation in the body was good and did not show any toxicity. Moreover, the limited observation depth does not result from a low efficiency or low concentration of the dye in the blood but results from optical absorption by brain tissues, which is important for blue dyes. Finally, the differences in the BBB permeability for compound **2** are not clear for the moment and would need further investigations which are behind the scope of the present paper.

DISCUSSION

Dyes **1** and **2** consist in two stilbenic units built around a biphenyl (for **1**) or 9,9′-dipropylfluorenyl (for **2**) central core. The fundamental difference between the two chromophores used here lies in the planar rigidity induced by the fluorenyl central core in **2**, in comparison with the free rotation that exists in the biphenyl central core in **1**. This rigidity induces excellent fluorescence efficiency even in water and hydrophobic environments for **2**.

The "J-aggregate" geometries in both chromophores lead to TPA cross-sections two orders of magnitude larger than commercial blue fluorophores (Anémian et al., 2002; Morel et al., 2001). The planar rigidity in **2** leads to an improved σ_2 TPA cross-section at 720 nm compared to **1**. The combination of the increase of σ_2 and fluorescence quantum yield of dye **2** improves by a factor 3 its TPEF detection limit in comparison to dye **1**. In addition, the *n*-propyl chains on the fluorenyl derivative **2** decrease the water solubility, but induce better lipid solubility in comparison with the biphenyl derivative **1**. This gives a decrease of the octanol–water partition coefficient log*P*. This structural modification can be generalized to lead to a fine tuning of log *P*. A better lipid solubility is an important property that facilitates the passage through cell membranes and BBB.

Both chromophores stain homogeneously the cytoplasm of cultured living cells within minutes. In the cytoplasm, both the dyes exhibit diffusion times and fluorescence characteristics that suggest their association with intracellular membranes. Moreover, their intracellular fluorescence decay is almost monoexponential, allowing FLIM imaging, in particular in co-staining with Hoechst 33342.

Thus, dye **2** appears as the best candidate for TPEF microscopies. In this work, we obtained TPEF images of living CHO cells with a good signal to noise ratio using laser powers in the sub-milliwatt range. These very low excitation powers are less invasive for living processes, and they reduce drastically the endogenous autofluorescence and photobleaching that may interfere with low-TPEF probes. For in vivo three-dimensional cerebral imaging, dye **2** opens the way for a blue labeling channel to study the cortex vasculature and extra vascular structures of nude mice at a depth of up to 200 μm.

In conclusion, we have reported here a general method of investigation of newly engineered TPEF dyes for in vivo two-photon microscopy with low-power excitation. This method has been successfully applied to the new blue fluorescent dyes **1** and **2** evidencing for one of these (**2**) the crossing of BBB. Finally, we observe that the chemical nature of dye **2** allows an easy functionalization for grafting various moieties such as chelators of heavy metals, which would be useful for X-rays photoactivation therapy or MRI imaging associated to two photon intravital microscopy.

ACKNOWLEDGMENTS

We thank CNRS and University Louis Pasteur of Strasbourg for financial support. Ali Hayek thanks French ministry MENESR for a PhD fellowship. Dr. Robert Pansu from ENS-Cachan is gratefully acknowledged for helpful discussions. The 2P microscopy and FLIM equipment (IAB, Grenoble) was financed by the Région Rhône-Alpes, MENESR, and Inserm.

REFERENCES

Abbotto A, Beverina L, Bozio R, Facchetti A, Ferrante C, Pagani GA, Pedron D, Signorini R. 2002. Novel heterocycle-based two-photon absorbing dyes. Org Lett 4:1495–1498.

Abbotto A, Baldini G, Beverina L, Chirico G, Collini M, D'Afonso L, Diaspro A, Magrassi R, Nardo L, Pagani GA. 2005. Dimethyl-pepep: a DNA probe in two-photon excitation cellular imaging. Biophys Chem 114:35–41.

Anémian R, Baldeck PL, Andraud C. 2002. Large two-photon absorption properties of polyphenyls and polyfluorenes. Mol Cryst Liq Cryst Sci Technol A 374:335–342.

Bousso P, Robey EA. 2004. Dynamic behavior of T cells and thymocytes in lymphoid organs as realed by two-photon microscopy. Immunity 21:349–355.

Göbel W, Kampa BM, Helmchen F. 2007. Imaging cellular network dynamics in three dimensions using fast 3D laser scanning. Nat Methods 4:73–79.

Grichine A, Feofanov A, Karmakova T, Kazachkina N, Pecherskih E, Yakubovskaya R, Mironov A, Egret-Charlier M, Vigny P. 2001. Influence of the substitution of 3-vinyl by 3-formyl group on the photodynamic properties of chlorin p6: molecular, cellular and in vivo studies. Photochem Photobiol 73:267–277.

Hayek A, Bolze F, Nicoud J-F, Baldeck PL, Mély Y. 2006. Synthesis and characterization of water-soluble two-photon excited fluorescent chromophores for bioimaging. Photobiol Photochem Sci 5:102–106.

Helmchen F, Denk W. 2005. Deep tissue two-photon microscopy. Nat Methods 2:932–940.

Imanishi Y, Batten M, Piston DW, Baehr W, Palczewski K. 2004. Noninvasive two-photon imaging reveals retinyl ester storage in the eye. J Cell Biol 164:373–383.

Krishna TR, Parent M, Werts MH, Moreaux L, Gmouh S, Charpak S, Caminade A-M, Majoral J-P, Blanchard-Desce M. 2006. Water-soluble dendrimeric two-photon tracers for in vivo imaging. Angew Chem Int Ed 45:4645–4648.

Miller MJ, Wei SH, Parker I, Cahalan MD. 2002. Two-photon imaging of lymphocite mobility and antigen response in intact lymph node. Science 296:1869–1873.

Morel Y, Irimia A, Najechalski P, Kervella Y, Stéphan O, Baldeck PL, Andraud C. 2001. Two-photon absorption and optical power limiting of bifluorene molecule. J Chem Phys 114:5391–5396.

Patterson GH, Piston DW. 2000. Photobleaching in two-photon excitation microscopy. Biophys J 78:2159–2162.

Serduc R, Vérant P, Vial J-C, Farion R, Rocas L, Rémy C, Fadlallah T, Brauer A, Bravin A, Laissue J, Blattmann H, van der Sanden B. 2006. In vivo two-photon microscopy study of short-term effects of microbeam irradiation on normal mouse brain microvasculature. Int J Radiat Oncol Biol Phys 64:1519–1527.

So PTC, Dong CY, Masters BR, Berland KM. 2000. Two-photon fluorescence microscopy. Annu Rev Biomed Eng 02:399–429.

Theer P, Denk W. 2006. On the fundamental imaging-depth limit in two-photon microscopy. J Opt Soc Am A Opt Image Sci Vis 23:3139–3149.

Vérant P, Serduc R, Van der Sanden B, Rémy C, Vial J-C. 2007. A direct method for measuring mouse capillary cortical blood volume using multiphoton laser scanning microscopy. J Cereb Blood Flow Metab 27:1072–1081.

Woo HY, Hong JW, Liu B, Mikhailovsky A, Korystov D, Bazan GC. 2005. Water-soluble [2.2]paracyclophane chromophores with large two-photon action cross sections. J Am Chem Soc 127:820–821.

Xu C, Williams RM, Zipfel W, Webb WW. 1996. Multiphoton excitation cross-sections of molecular fluorophores. Bioimaging 4:198–207.

Zipfel WR, Williams RM, Webb WW. 2003. Nonlinear magic: multiphoton microscopy in the bioscience. Nat Biotech 21:1369–1375.